

Experimental validation of demand side response rates for frequency control

Leo Casasola-Aignesberger*, Friedrich Wiegel†, Simon Waczowicz†, Veit Hagenmeyer† and Sergio Martinez*

*Department of electrical engineering, Escuela Técnica Superior de Ingenieros Industriales, Universidad Politécnica de Madrid, Madrid, Spain

Email: leo.casasola@upm.es, sergio.martinez@upm.es

†Institute for Automation and Applied Informatics, Karlsruhe Institute of Technology (KIT)

Email: friedrich.wiegel@kit.edu, simon.waczowicz@kit.edu, veit.hagenmeyer@kit.edu

Abstract—Renewable energy generation is replacing conventional synchronous generators in electrical power systems around the world. A side effect of this trend is a reduction in system inertia and the power available for frequency control. In this study, the authors investigate an island power system of interest under different conditions with varying levels of demand side response penetration and analyze its impact on frequency behavior. The obtained simulation results are then complemented with a series of experiments carried out using a combination of real hardware and Power-Hardware-In-the-Loop equipment, to test the validity and limitations of the simulation results. In summary, demand side response can notably improve the frequency response of an island power system, but excessive demand side response leads to unacceptable frequency oscillations.

Index Terms—Frequency control, renewable energy sources, decentralized demand side participation, reduced inertia

I. INTRODUCTION

The effects of large-scale integration of renewable generation in insular electrical power systems are diverse [1]–[4], ranging from their lack of dispatchability to their impact on power flows. In particular, the current paper examines the frequency fluctuations caused by wind turbines due to variations in wind speed. The lack of inertia in converter-interfaced renewable sources, such as full-converter wind turbines, has led to frequency control issues [5] and increased curtailed energy, which has significant economic and environmental consequences [6].

Two approaches have been proposed in the literature to address this issue: improving the performance of the generation side [7], or adapting the consumption side [8]. On the generation side, advanced control techniques applied to the power electronics of wind turbines allow their output power to be adjusted [9]. On the demand side, an important research area is coordinating the large number of loads needed to make a significant contribution [10], as well as finding ways to aggregate these demands [11] and modeling the loads [12].

To improve frequency stability, this paper proposes a decentralized demand side response (DSR) mechanism to support conventional frequency control without the need for further communication [13]. Can DSR contribute to frequency control? Are there any limits to this contribution? This paper presents the results of a set of simulations which have then

been tested in an experimental setup in the facilities of Energy Lab 2.0 at KIT [14].

The rest of this paper is structured as follows: section II describes the scenarios analyzed and the proposed DSR strategy; section III presents the simulation results; section IV describes the setup used for the experimental validation, and section V presents experimental results. Finally, section VI presents the conclusions of this work.

II. DEMAND SIDE RESPONSE AND SCENARIOS

The system consists of a synchronous generator, a wind turbine, smart loads and passive loads as shown in figure 1. All passive elements, such as lines or transformers, are not being considered.

- The synchronous generator (SG) provides part (or all) of the power, and also performs frequency control.
- The wind turbine generator (WTG) can provide part of the demanded power, without participating in frequency control.
- The loads can be categorized in two groups:
 - Passive loads: These loads demand most of the power and do not react to frequency deviations.
 - Smart loads: These loads can respond to frequency deviations, varying their power demand. This is referred to as Demand Side Response (DSR).

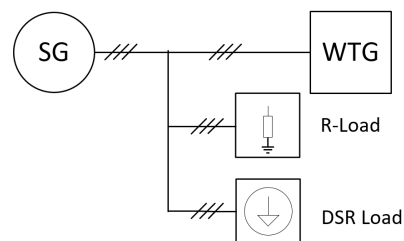


Fig. 1: Diagram of the simplified power system

A. Scenarios

Two distinct scenarios have been considered to assess the impact of DSR on frequency response:

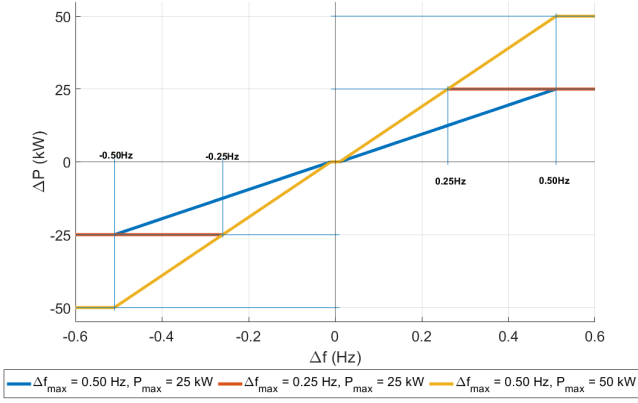


Fig. 2: Proposed DSR strategy examples

1) *Step disturbance*: the response of the system is analyzed when a step load is applied, without wind generation. Its implementation is described in algorithm 1.

2) *Wind perturbations*: the power output from the wind turbine varies according to the incident wind profile [15]. This induces frequency fluctuations which activate the DSR mechanism. Its implementation is described in algorithm 2.

Algorithm 1 Step scenarios pseudo-code

```

initializeSystem
for  $P_{DSR} = [400, 800, 1600, 3200, 6400]$  do ▷ (in W)
  for  $\Delta f_{max} = [0.125, 0.250, 0.375, 0.500]$  do ▷ (in Hz)
    powerDemand += 5 kW ▷ step in demand (up)
    delay(30s) ▷ wait for steady state
    powerDemand -= 5kW ▷ step in demand (down)
  end for
end for

```

Algorithm 2 Wind scenario pseudo-code

```

for  $P_{DSR} = [400, 800, 1600, 3200, 6400]$  do ▷ (in W)
  for  $\Delta f_{max} = [0.125, 0.250, 0.375, 0.500]$  do ▷ (in Hz)
    initializeSystem
    start wind profile
    end case
  end for
end for

```

B. Demand Side Response strategy

The DSR strategy has already been presented in detail [13], [16], [17], so only a brief description will be included. It consists of a linear adaptation of the demanded power to the locally measured frequency (Fig. 2). Two values have to be considered: the maximum power deviation (referred to as P_{DSR}) and the frequency deviation value for which the full power deviation is reached (referred to as Δf_{max}), which will be the parameters in each case.

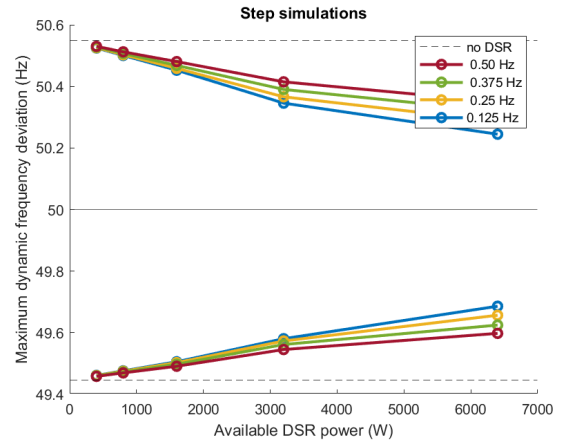


Fig. 3: Frequency deviation for the step scenarios

III. SIMULATION RESULTS

All simulations presented here have been carried out in *Matlab/Simulink*, using the *Specialized Power System Library* [18], as presented in [16], [17].

A. Step disturbance

The base scenario consists of a total demand of 30 kW supplied entirely by a synchronous generator, and a 5 kW step disturbance in demand. The metric used to compare the different scenarios is the frequency deviation.

The general results of these scenarios are summarized in figure 3. It shows that as the DSR increases, the value of the frequency deviation decreases. It is noted that the influence of Δf_{max} is significant only for sufficient P_{DSR} . For example, all cases with $P_{DSR} = 0.4$ kW (a very low value) have the same frequency deviations (Fig. 3). The frequency deviation values for the scenario with no DSR is provided as a base case for comparison.

Figure 4 shows the frequency evolution for different cases just after a sudden decrease in the demanded power. As expected, higher values of P_{DSR} (for a given value of Δf_{max}) lead to smaller values of frequency deviations.

However, the case with $P_{DSR} = 6.4$ kW and $\Delta f_{max} = 0.25$ Hz stands out in an unexpected way: the frequency no longer presents a smooth behavior, but small and fast frequency oscillations can be observed (green line in figure 4). To further expose this phenomenon, the frequency evolution for the cases with $\Delta f_{max} = 0.125$ Hz are presented in figure 5. This graph shows unacceptable frequency behavior with excessive demand side response in the form of notable fast frequency oscillations, with a frequency around 30 Hz. In this scenario, consisting only of a single disturbance of significant size (5 kW over a total of 30 kW demand), the frequency does eventually regain its smooth behavior.

B. Wind disturbances

In order to analyze the influence of demand side response in a more realistic situation, an additional scenario has been

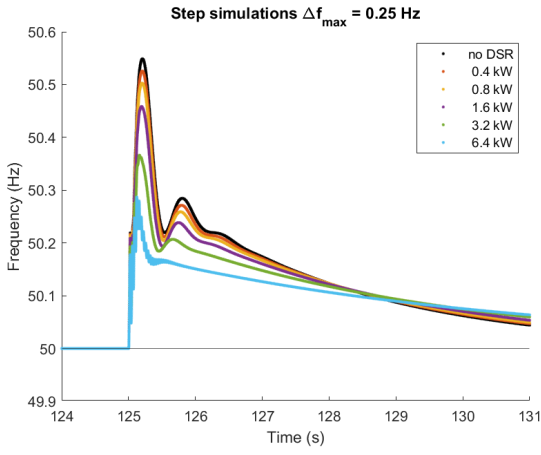


Fig. 4: Frequency evolution for a 5 kW step, for $\Delta f_{max} = 0.25 Hz$ and different values of available P_{DSR}

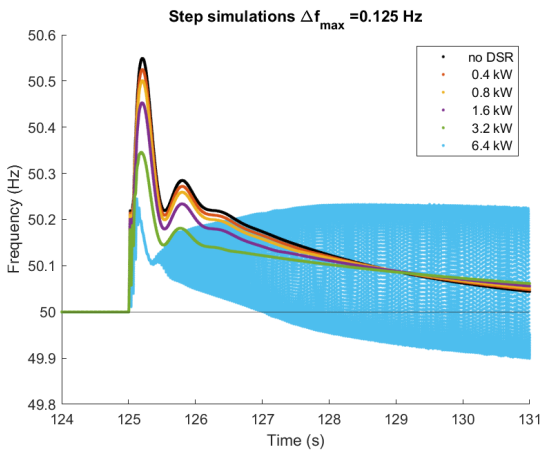


Fig. 5: Frequency evolution in an edge case: a 5 kW step with different values of P_{DSR} , at $\Delta f_{max} = 0.125 Hz$

considered, where part of the generation comes from wind power, which is exposed to a variable wind profile, and is the cause of the frequency deviations. The wind profile used has been obtained from [15], consists of data recorded at Tjæreborg (Denmark) at 60m above ground and a sample rate of 25 s.p.s. It has an average wind speed of 10 m/s and high variability, with a *Turbulent Index* of 17%.

The results for the simulations of this scenario are summarized in figures 6 and 7. The first aspect that stands out is that the fast frequency oscillation cases are clearly noticeable. For the other cases, it is noted that the trend observed in the step simulations persists: more DSR improves frequency behavior.

Figure 8 shows a detail of the frequency behavior for the cases with $\Delta f_{max} = 0.375 Hz$, and no abnormal behavior of the frequency can be seen. It shows that, just as in the step scenario, more DSR leads to smaller frequency deviations.

Figure 9 shows the cases with excessive demand side response, where the frequency presents fast oscillations as

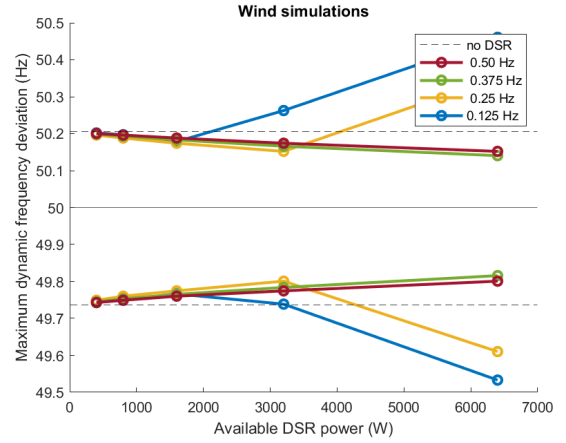


Fig. 6: Extreme frequency deviations for the wind simulations

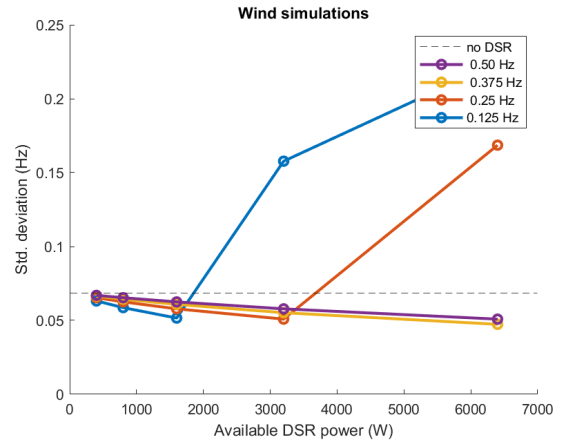


Fig. 7: Standard deviation of frequency in the wind simulations

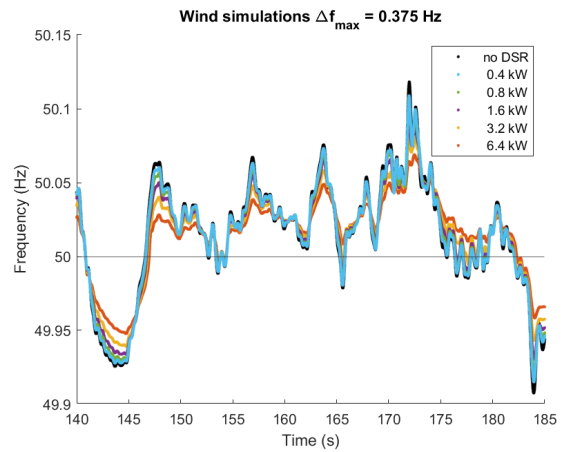


Fig. 8: Frequency evolution for the selected wind profile, at a response rate of $\Delta f_{max} = 0.375 Hz$ and different available P_{DSR} values

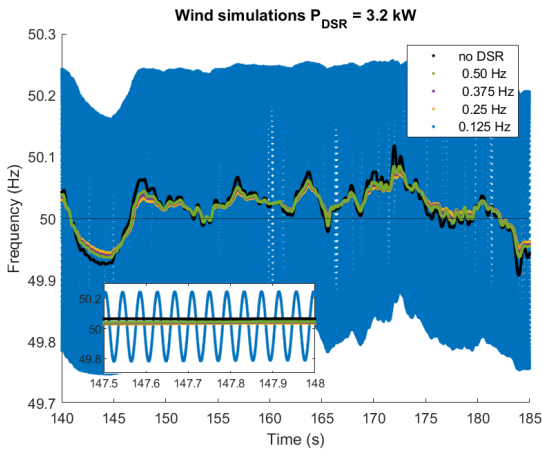


Fig. 9: Frequency evolution for the selected wind profile, with 3200 W of available P_{DSR} at different response rates

well. The miniature in figure 9 shows a close-up view of the oscillations, which present an amplitude of 0.4 Hz and a frequency of 24 Hz. It is noted that in this scenario, the cases with $P_{DSR} = 3.2 \text{ kW}$ and $\Delta f_{max} = 0.125 \text{ Hz}$, and $P_{DSR} = 6.4 \text{ kW}$ and $\Delta f_{max} = 0.250 \text{ Hz}$ present these frequency oscillations as well as the case with $P_{DSR} = 6.4 \text{ kW}$ and $\Delta f_{max} = 0.125 \text{ Hz}$ in the step scenario.

These simulations show that DSR has the potential to positively contribute to frequency behavior in this system, but under certain circumstances can lead to fast frequency oscillations and unacceptable frequency behavior. In order to validate these results, a series of experiments have been carried out and are described in section IV.

IV. EXPERIMENTAL SETUP

To validate the demand response strategies proposed in this article and to assess their feasibility, the experimental setup of the Energy Lab 2.0 at KIT was used. The Smart Energy System Control Laboratory (SESSL) provides a platform for such experiments [19]. As presented in [6], several real elements as well as two power hardware-in-the-loop (PHIL) systems can be combined in a generic and on-the-fly adjustable topology to simulate various low-voltage (LV) power grids. In this particular case, a synchronous generator, a controllable resistive load, and two PHIL systems were interconnected via a busbar, as shown in Figure 1, to provide the system topology of interest. The main parameters of each component used and their role in the experiment are summarized below:

- Self-excited four pole synchronous generator with the nominal power of 56 kVA acts as the main power source, while providing conventional PI-controller based voltage and frequency regulation. The gain factors $K_p = 0.01$ and $K_i = 0.05$ of the frequency control were adjusted in such a way that the frequency response of the generator approximates as closely as possible the frequency response from the simulation with an identical load step.

- The base load of the system in the amount of 20 kW is provided by a controllable resistive load.
- Taking advantage of the flexibility of the PHIL units, they are used to (1) provide a variable speed wind turbine and (2) mimic the smart load with the behavior described in Section II according to the desired profile, taking part in frequency control. Since the wind turbine is not the subject of the study and is primarily intended to contribute only to the variable power behavior within the System-Under-Test (SUT), it is modeled as a grid-following current source to simplify the overall complexity. Within the model, the wind profile is scaled to the nominal system power and the power is fed into the grid according to the wind profile.

The utilized PHIL system is formed by digital four-quadrant amplifier CSU100 2GAMP4 from Egston and real-time simulator OP5707 from OPAL-RT.

Both WTG and smart load instances use the ideal-transformer-method (ITM) [20] as an interface algorithm between the SUT and the real-time simulation model. To be more precise, the closed-loop PHIL interface to the SUT is stabilized using first-order low-pass filters in the feedback path with a comparatively high cut-off frequency (2 kHz) relative to the frequency of interest (50 Hz fundamental) to assure stability while retaining PHIL accuracy.

V. EXPERIMENTAL RESULTS

The same scenarios that have been previously presented after simulation, have been reproduced experimentally. Due to the experimental nature of these results, the data is inherently less smooth, as will be evident in the figures in this section. Furthermore, some short intervals are missing due to limitations in the data capture device. However, enough experiments have been conducted to gather all relevant data.

As a reminder, the focus of the experiments is on the main objectives, which are:

- Validate the relative improvement of frequency behavior with varying P_{DSR} and Δf_{max} .
- Confirm or dismiss the appearance of fast frequency oscillations when excessive DSR is present.

A. Step disturbance

Figure 10 summarizes the results of the step experiments: for the studied scenarios, the effect of increasing P_{DSR} seems to be more significant than the variation of Δf_{max} , and increasing DSR leads to smaller frequency deviations.

Figure 11 shows the frequency for scenarios with $\Delta f_{max} = 0.25 \text{ Hz}$, equivalent to figure 4 in section III, for a sudden 5kW drop in demand at the instant $t = 70 \text{ s}$. It confirms the findings of the simulations, as increasing values of P_{DSR} lead to smaller frequency deviations. Furthermore, just as observed in the simulation results, the most extreme case with $P_{DSR} = 3.2 \text{ kW}$ and $\Delta f_{max} = 0.25 \text{ Hz}$ presents suspicious frequency oscillations, although in the experimental results they are less clear due to the inherent variation of the frequency even in steady state, and seem to have a frequency of around 3 Hz,

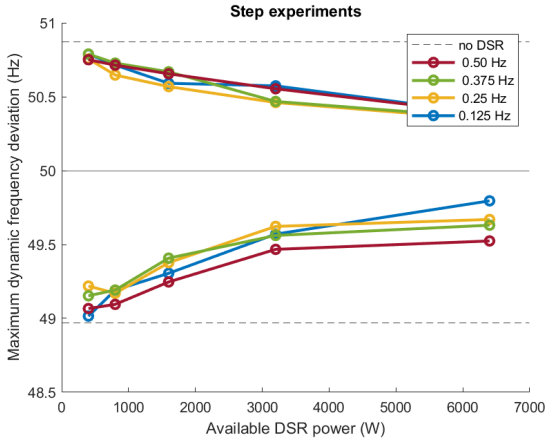


Fig. 10: Extreme frequency deviations for the step experiments

different from those observed in the simulations (30 Hz). This remains an open topic, seemingly related to the limitations of the model, and will be addressed in future research.

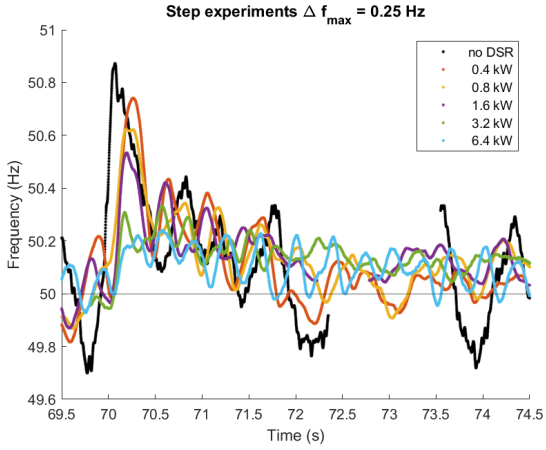


Fig. 11: Frequency evolution for a 5 kW step at $\Delta f_{max} = 0.25 Hz$ and different values of available DSR.

B. Wind disturbances

Figures 12 - 13 summarize the experimental results for the wind scenarios. Just as in the simulations, these results show an improvement on the frequency behavior with increasing demand side participation. It is noted that the frequency oscillations are not detected with these metrics.

Figure 14 shows an extract of the frequency evolution for different values of P_{DSR} with $\Delta f_{max} = 0.50 Hz$. It stands out that, for the case with $P_{DSR} = 6.4 kW$, the frequency shows a clear oscillation (with about 0.1 Hz amplitude and 30 Hz frequency) that is not present in the other cases.

VI. CONCLUSIONS

Demand side response offers great potential for contributing to frequency control, but presents its own set of challenges in managing its participation. The results presented here show

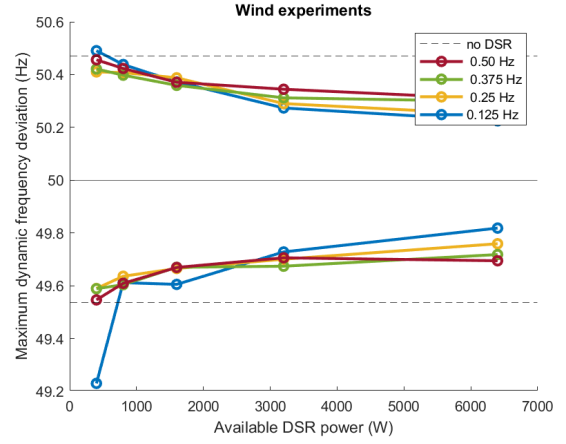


Fig. 12: Extreme frequency deviations for wind experiments

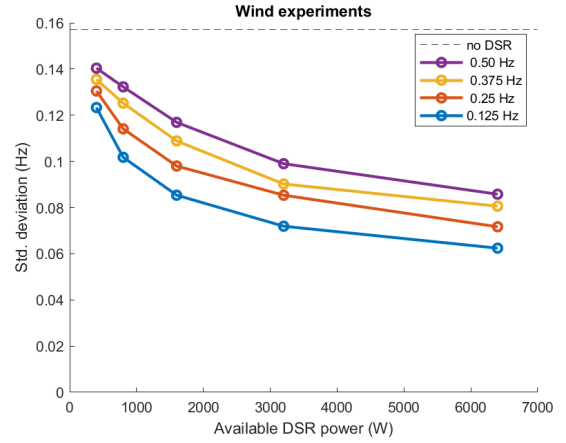


Fig. 13: Frequency standard deviation in wind experiments

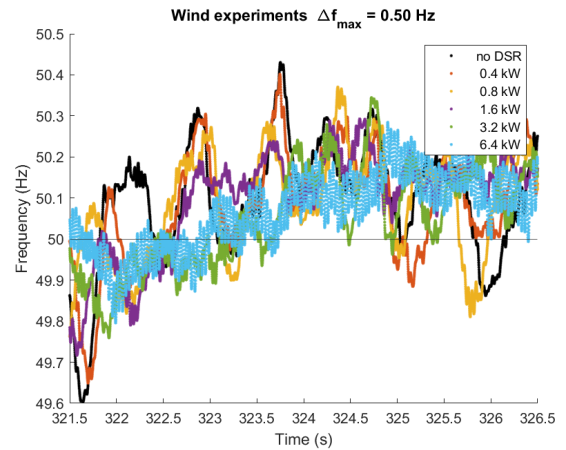


Fig. 14: Extract of the frequency evolution for the proposed wind scenario, with $\Delta f_{max} = 0.50 Hz$

the value of simulations, the importance of accurate modeling and the validation of simulation results in a realistic setup with real hardware.

The results of the simulations show that DSR can reduce frequency deviations, reduce the frequency nadir at sudden demand changes, and improve the frequency behavior when wind power contributes significantly to power generation. The main result here is, as expected, that more available power participating in demand side response leads to more stable frequency. However, if the DSR is too impetuous, frequency oscillations occur that would be unacceptable in a real scenario.

The experiments carried out to verify these simulations roughly agree with the benefits of DSR on frequency behavior, and partially confirm the oscillations: although some oscillations were observed in the experiments, they do not completely resemble the simulated ones neither in frequency nor in amplitude, nor in the cases in which they occur. These oscillations resemble the behavior of a P-controller with excessive gain, but further research on this topic is pending, including an analytical approach, to explore the limitations of the model and test the significance of the experiments.

REFERENCES

- [1] E. M. G. Rodrigues, A. W. Bizuayehu, and J. P. S. Catalao, "Analysis of requirements in insular grid codes for large-scale integration of renewable generation," in *2014 IEEE PES T&D Conference and Exposition*, (Chicago, IL, USA), pp. 1–5, IEEE, Apr. 2014.
- [2] D. Ochoa and S. Martinez, "Frequency Control Issues in Power Systems: the Effect of High Share of Wind Energy," *IEEE Latin America Transactions*, vol. 16, pp. 1934–1944, July 2018.
- [3] F. Milano, F. Dorfler, G. Hug, D. J. Hill, and G. Verbic, "Foundations and Challenges of Low-Inertia Systems (Invited Paper)," in *2018 Power Systems Computation Conference (PSCC)*, (Dublin), pp. 1–25, IEEE, June 2018.
- [4] H. Ibrahim, M. Ghandour, M. Dimitrova, A. Ilinca, and J. Perron, "Integration of Wind Energy into Electricity Systems: Technical Challenges and Actual Solutions," *Energy Procedia*, vol. 6, pp. 815–824, 2011.
- [5] D. Ochoa and S. Martinez, "Frequency Control Issues in Power Systems: the Effect of High Share of Wind Energy," *IEEE Latin America Transactions*, vol. 16, pp. 1934–1944, July 2018.
- [6] C. Jauch, *Stability and Control of Wind Farms in Power Systems*. 2006.
- [7] N. K. Roy, S. Islam, A. K. Podder, T. K. Roy, and S. M. Mueen, "Virtual Inertia Support in Power Systems for High Penetration of Renewables—Overview of Categorization, Comparison, and Evaluation of Control Techniques," *IEEE Access*, vol. 10, pp. 129190–129216, 2022.
- [8] S. Tripathi, V. P. Singh, N. Kishor, and A. Pandey, "Load frequency control of power system considering electric Vehicles' aggregator with communication delay," *International Journal of Electrical Power & Energy Systems*, vol. 145, p. 108697, Feb. 2023.
- [9] B. Spichartz, K. Gunther, and C. Sourkounis, "New Stability Concept for Primary Controlled Variable Speed Wind Turbines Considering Wind Fluctuations and Power Smoothing," *IEEE Transactions on Industry Applications*, vol. 58, pp. 2378–2388, Mar. 2022.
- [10] T. Jiang, P. Ju, C. Wang, H. Li, and J. Liu, "Coordinated Control of Air-Conditioning Loads for System Frequency Regulation," *IEEE Transactions on Smart Grid*, vol. 12, pp. 548–560, Jan. 2021.
- [11] H. Liu, Z. Hu, Y. Song, and J. Lin, "Decentralized Vehicle-to-Grid Control for Primary Frequency Regulation Considering Charging Demands," *IEEE Transactions on Power Systems*, vol. 28, pp. 3480–3489, Aug. 2013.
- [12] N. Neofytou, K. Blazakis, Y. Katsigiannis, and G. Stavrakakis, "Modeling Vehicles to Grid as a Source of Distributed Frequency Regulation in Isolated Grids with Significant RES Penetration," *Energies*, vol. 12, p. 720, Feb. 2019.
- [13] L. Casasola-Aignesberger and S. Martinez, "Decentralized Demand Side Participation in Primary Frequency Control: Assessing the Impact of Response Rates," *IEEE Access*, vol. 11, pp. 31977–31989, 2023.
- [14] "Smart Energy System Control Laboratory (SESCL)," <https://www.iai.kit.edu/english/RPE-SESCL.php>.
- [15] K. S. Hansen and G. C. Larsen, "Database of wind Characteristics (DTU - Department of Wind energy)," <http://winddata.com/>.
- [16] L. Casasola-Aignesberger and S. Martinez, "Fast frequency oscillations detection in low inertia power systems with excessive demand-side response for frequency regulation," in *Renewable Energy and Power Quality Journal*, vol. 19, (Almería, Spain), pp. 557–560, July 2021.
- [17] L. Casasola-Aignesberger and S. Martinez, "Electric vehicle recharge strategies for frequency control in electrical power systems with high wind power generation," in *2020 IEEE International Conference on Environment and Electrical Engineering and 2020 IEEE Industrial and Commercial Power Systems Europe (EEEIC/ICPS Europe)*, pp. 1–5, June 2020.
- [18] "MATLAB and Simscape Power Systems Toolbox, release 2018b." The MathWorks, Inc., 2018.
- [19] F. Wiegel, J. Wachter, M. Kyesswa, R. Mikut, S. Waczowicz, and V. Hagenmeyer, "Smart Energy System Control Laboratory – a fully-automated and user-oriented research infrastructure for controlling and operating smart energy systems," *at - Automatisierungstechnik*, vol. 70, no. 12, pp. 1116–1133, 2022.
- [20] G. Tanuku, K. S. Amitkumar, J.-N. Paquin, S. A. R. Naqvi, and R. Venugopal, "Ideal Transformer Method Optimization for Power Hardware-in-the- Loop Simulations of Grid Connected Inverters," *PCIM Europe 2022: International Exhibition and Conference for Power Electronics, Intelligent Motion, Renewable Energy and Energy Management*, 2022.